Interactions of Remote Alkyl Groups with Lanthanide Metal Centers: Synthesis, Characterization and Ligand Redistribution Reactions of Heterobimetallic Species Containing Trialkylaluminum Fragments

Garth R. Giesbrecht,[a] John C. Gordon,*[b] John T. Brady,[b] David L. Clark,[c] D. Webster Keogh,[b] Ryszard Michalczyk,[d] Brian L. Scott,[b] and John G. Watkin[b]

Keywords: Lanthanides / Samarium / Aluminum / O ligands / Agostic interactions

The reaction of $[Ln(OAr)_3]_2$ with four equivalents of trialkylaluminum leads to the formation of the bis-trialkylaluminum adducts $(ArO)Ln[(\mu\text{-}OAr)(\mu\text{-}R)AlR_2]_2$ [Ln = La, R = Me (**1**); Ln = La, R = Et (**3**); Ln = Sm, R = Et (**4**)]. The X-ray crystal structure of **1** reveals short La–C(bridging) distances of 2.800(5) and 2.759(5) Å. A reduced $^1J_{C\text{-}H}$ coupling constant of 110 Hz and a low energy ν(C–H) stretch in the solution and solid state IR spectra are consistent with a strong agostic La···H–C interaction in solution. Crystal data for **1**: a = 11.708(2) Å; b = 18.416(4) Å; c = 20.949(4) Å; α = 90°; β = 90°; γ = 90°; V = 4516.8(15) Å^3; Z = 4; $R1$ = 4.69%. The solid-state structure of the samarium ethyl derivative **4** reveals close contacts of 2.627(4) and 2.649(4) Å between the samarium center and the methylene carbons of the triethylaluminum groups. The room temperature ^{13}C NMR spectrum of **4** exhibits a $^1J_{C\text{-}H}$ coupling constant of 102 Hz; additionally, the fluxional process that exchanges methyl groups in **1** and **2** is slow enough on the NMR time scale to allow distinct methylene groups in **4** to be observed. Crystal data for **4**: a = 19.318(1) Å; b = 20.150(1) Å; c = 26.280(1) Å; α = 90°; β = 90°; γ = 90°; V = 10229.8(9) Å^3; Z = 8; $R1$ = 3.53%. Thermolysis of **1**–**4** results in ligand redistribution to form $[R_2Al(OAr)]_2$ [R = Me, Et (**5**)] and other unidentified species. Crystal data for **5**: a = 9.496(4) Å; b = 10.183(4) Å; c = 18.794(7) Å; α = 90.06(1)°; β = 92.394(7)°; γ = 114.976(6)°; V = 1645.6(11) Å^3; Z = 2; $R1$ = 10.13%.

Introduction

Aryloxide groups have proven to be suitable ancillary ligands in organolanthanide chemistry due in part to their ability to participate in π-bonding with electron-deficient metal centers.[1−3] Additionally, the coordination number and degree of oligomerization may be controlled through the use of bulky substituents on the arene ring. For example, use of the sterically demanding aryloxide ligand 2,6-di-*tert*-butyl-4-MeC_6H_2 leads to the formation of mononuclear complexes $Ln(OAr)_3$ for the entire lanthanide series.[4] Although these complexes are three-coordinate, they are essentially inert, with their reaction chemistry being limited to adduct formation with Lewis bases [i.e. $Ln(OAr)_3L$].[5] Previously, we demonstrated that the smaller 2,6-diisopropylphenoxide ligand bridges between metal centers in an unusual η^6-bridging mode to alleviate the steric unsaturation at the metal center.[1] Addition of a Lewis base to these complexes (e.g. THF, NH_3) leads to the formation of five-, six- or seven-coordinate species,[2] illustrating the large effect that a relatively small change in the steric bulk of the ancillary ligand may have upon a simple process such as adduct formation.

Recent studies of lanthanide alkoxide and aryloxide complexes have revealed that heterobimetallic complexes can often be obtained by utilizing the tendency of $^-$OR and $^-$OAr ligands to bridge two different metals.[6−10] Heterobimetallic complexes of the lanthanide metals (particularly when aluminum is one component) are of interest with respect to a) catalysis[11−13] and b) in the production of mixed-metal solid-state materials (e.g. lanthanide-doped ceramics) which may exhibit unusual and interesting physical properties.[14−18] In light of these reports, we were interested in exploring the reaction of these π-arene-bridged dimers with Lewis acids such as $AlMe_3$. Recently, we reported the solid state and solution properties of the mixed-metal complex $(ArO)Sm[(\mu\text{-}OAr)(\mu\text{-}Me)AlMe_2]_2$ (Ar = 2,6-*i*$Pr_2C_6H_3$) which maintains a strong agostic Sm···H−C interaction

[a] Nuclear Materials Technology Division, Los Alamos National Laboratory,
Los Alamos, New Mexico 87545, USA
[b] Chemistry Division, Los Alamos National Laboratory,
Los Alamos, New Mexico 87545, USA
Fax: (internat.) +1-505/667-9905
E-mail: jgordon@lanl.gov
[c] Glenn T. Seaborg Institute for Transactinium Science, Los Alamos National Laboratory,
Los Alamos, New Mexico 87545, USA
[d] Bioscience Division, Los Alamos National Laboratory,
Los Alamos, New Mexico 87545, USA

in solution.[19] However, the paramagnetism of trivalent samarium precluded a detailed study of this compound by ^1H and ^{13}C NMR spectroscopy. Thus, we sought to synthesize the diamagnetic lanthanum derivative in order to further investigate the nature of any fluxional processes that may be occurring in solution. Additionally, we were interested in the effect of introducing a larger Lewis acid into the coordination sphere (i.e. $AlEt_3$). Here we describe the synthesis and characterization of heterobimetallic complexes of lanthanum and samarium, and suggest that the solid-state structures of these agostic complexes may be viewed as potential "snapshots" of the intermediates present in the alkylation reaction of a lanthanide metal with trialkylaluminum reagents.

Results and Discussion

The addition of four equivalents of trimethyl- or triethylaluminum to a toluene solution of the π-arene bridged dimers $[Ln(OAr)_3]_2$ (Ar = 2,6-*i*$Pr_2C_6H_3$) (Ln = La, Sm)[1,2] yields the bis-trialkylaluminum adducts (ArO)Ln[(μ-OAr)(μ-R)$AlR_2]_2$ [Ln = La, R = Me (**1**); Ln = Sm, R = Me (**2**); Ln = La, R = Et (**3**); Ln = Sm, R = Et (**4**)] [Equation (1)].

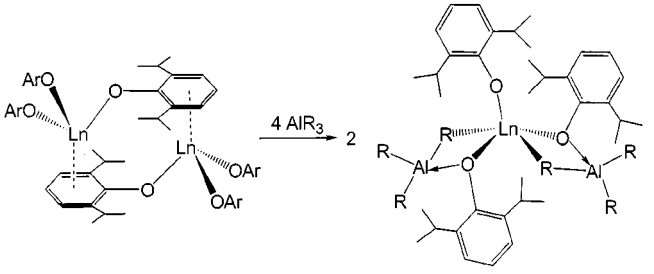

(1)

The trimethylaluminum adducts were isolated as colorless (La) and orange (Sm) solids in good yield. Complexes **1**−**4** are soluble in common organic solvents such as hexane and toluene. A measure of the crowding around the lanthanide center is given by the complexation of only two molecules of $AlMe_3$ or $AlEt_3$ per metal. In the reaction of $[Ln(OAr)_3]_2$ with six equivalents of AlR_3 only the bis-aluminum complex was isolated {and not Ln[(μ-OAr)(μ-R)-$AlR_2]_3$ as is observed for smaller alkoxide groups such as O*t*Bu (M = Y, Pr, Nd).[8,9]}

Single crystals of (ArO)La[(μ-OAr)(μ-Me)$AlMe_2]_2$ (**1**) were obtained by slow evaporation of a saturated toluene solution. An ORTEP view of the molecular structure is given in Figure 1; selected bond lengths and angles are given in Table 1. Complete details of the structural analyses of compounds **1**, **4** and $[Et_2Al(OAr)]_2$ (**5**) are presented in Table 4.

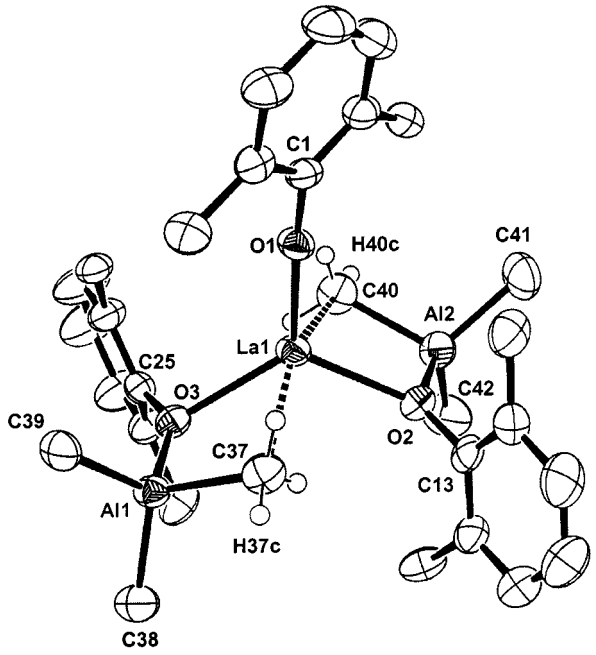

Figure 1. ORTEP view of (ArO)La[(μ-OAr)(μ-Me)$AlMe_2]_2$ (**1**) drawn with 30% probability ellipsoids; isopropyl methyl groups have been omitted for clarity

Table 1. Selected bond lengths (Å) and angles (deg) for (ArO)La-[(μ-OAr)(μ-Me)$AlMe_2]_2$ (**1**)

La1−O1	2.136(3)	La1−O2	2.387(3)
La1−O3	2.367(3)	La1−C37	2.800(5)
La1−C40	2.759(5)	O1−C1	1.369(5)
O2−C13	1.403(5)	O3−C25	1.386(4)
O2−Al2	1.864(3)	O3−Al1	1.848(3)
Al1−C37	2.040(5)	Al1−C38	1.969(5)
Al1−C39	1.967(5)	Al2−C40	2.053(6)
Al2−C41	1.964(6)	Al2−C42	1.963(6)
O1−La1−O2	116.16(11)	O1−La1−O3	120.72(11)
O1−La1−C37	99.27(15)	O1−La1−C40	102.87(16)
O2−La1−O3	122.01(10)	O2−La1−C37	93.70(13)
O2−La1−C40	69.82(15)	O3−La1−C37	67.56(12)
O3−La1−C40	106.43(14)	C37−La1−C40	156.62(16)
La1−O1−C1	175.2(3)	La1−O2−C13	125.4(2)
La1−O3−C25	108.1(2)	La1−O2−Al2	104.09(14)
La1−O3−Al1	107.31(12)	La1−C37−H37c	172(3)
La1−C40−H40c	177(4)		

The structure of **1** is isomorphous with that previously reported for the samarium derivative **2**. Both trimethylaluminum adducts crystallize in the orthorhombic space group $P2_12_12_1$ with equivalent unit cell parameters. As found for **2**, the geometry about the metal center is square-based pyramidal, with a terminal aryloxide ligand occupying the apical site and two [(μ-OAr)(μ-Me)$AlMe_2$] units in the basal plane of the molecule. The La−C distances of 2.800(5) and 2.759(5) Å are slightly longer than the Sm−C distances observed in **2** [2.620(5) and 2.632(5) Å] and reflect both the larger size of lanthanum and a weaker agostic Ln···H−C interaction.[20] By comparison, these bond lengths are longer than the La−C σ bonds in La[$CH(SiMe_3)_2]_3$

[2.515(9) Å][21] or (η^5-C_5Me_5)La[$CH(SiMe_3)_2$]$_2$ [2.537(5) and 2.588(4) Å][22] but similar to the Nd−C(bridging) distance reported in Nd[(μ-O*t*Bu)(μ-Me)$AlMe_2$]$_3$ (2.784 (11) Å].[9] A feature common to the crystal structures of **1**, **2** and **4** is the presence of two distinct types of lanthanide-oxygen bonds; the two longer bonds [2.387(3) and 2.367(3) Å in **1**] are a result of the interaction of the AlR_3 groups with the phenoxide oxygen atoms (i.e. there is a competition between two Lewis acid centers for the oxygen electron density). The third unique phenoxide ligand "compensates" for the electron-deficient nature of the lanthanide center by engaging in O→M π-bonding, as evidenced by the very short Ln−O distance [2.136(3) Å] and the almost linear La−O−C angle [175.2(3)°]. The hydrogen atoms on C37 and C40 were located and refined and define a trigonal bipyramidal geometry for these carbon atoms. The lanthanum center and H37c and H40c occupy the axial positions [La1−C37−H37c = 172(3)°, La1−C40−H40c = 177(4)°] with the aluminum center and the remaining hydrogen atoms in the equatorial positions. As was found for **2**, the hydrogen atoms do not point directly towards the lanthanide center, which supports a β-Al−C···La type of interaction in which electron density from the aluminum-carbon bond is donated to the metal center.[23,24] Consistent with this postulate is the observation of elongated $Al-C_{agostic}$ bonds [2.040(5) and 2.053(6) Å]; these bond lengths are about 0.1 Å longer than the remaining Al−C bonds in **1** [1.969(5) to 1.964(6) Å]. Overall, the metrical parameters of **1** are similar to those determined for the samarium derivative **2**, with the significant features of an agostic Ln···H−C interaction being present in both.

Orange crystals of (ArO)Sm[(μ-OAr)(μ-Et)$AlEt_2$]$_2$ (**4**) that were amenable to X-ray crystal diffraction were obtained by slow evaporation of a saturated hexamethydisiloxane solution. The molecular structure of **4** is shown in Figure 2 with a list of important bond lengths and angles available in Table 2.

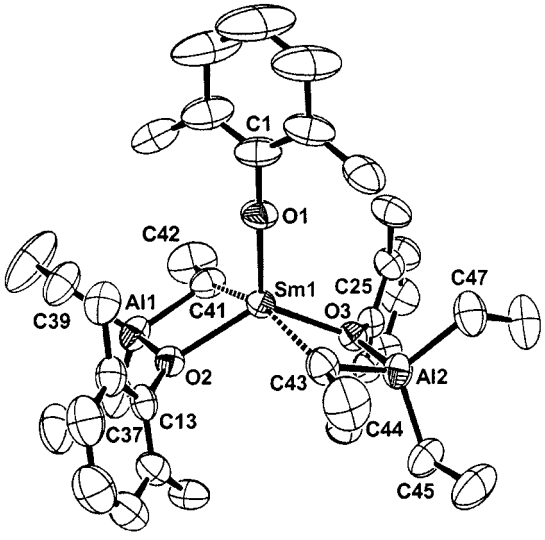

Figure 2. ORTEP view of (ArO)Sm[(μ-OAr)(μ-Et)$AlEt_2$]$_2$ (**4**) drawn with 30% probability ellipsoids; isopropyl methyl groups have been omitted for clarity

Table 2. Selected bond lengths (Å) and angles (deg) for (ArO)Sm[(μ−OAr)(μ-Et)$AlEt_2$]$_2$ (**4**)

Sm1−O1	2.060(2)	Sm1−O2	2.292(2)
Sm1−O3	2.295(2)	Sm1−C41	2.627(4)
Sm1−C43	2.649(4)	O1−C1	1.376(4)
O2−C13	1.404(4)	O3−C25	1.408(4)
O2−Al1	1.877(2)	O3−Al2	1.875(2)
Al1−C37	1.963(4)	Al1−C39	1.975(4)
Al1−C41	2.067(4)	Al2−C43	2.055(4)
Al2−C45	1.966(4)	Al2−C47	1.976(4)
O1−Sm1−O2	117.18(8)	O1−Sm1−O3	118.33(8)
O1−Sm1−C41	97.52(11)	O1−Sm1−C43	102.30(11)
O2−Sm1−O3	124.49(7)	O2−Sm1−C41	72.37(10)
O2−Sm1−C43	97.10(10)	O3−Sm1−C41	99.85(10)
O3−Sm1−C43	71.80(10)	C41−Sm1−C43	160.14(12)
Sm1−O1−C1	178.0(2)	Sm1−O2−C13	124.81(17)
Sm1−O3−C25	126.12(17)	Sm1−O2−Al1	103.60(9)
Sm1−O3−Al2	103.88(10)	Sm1−C41−C42	166.8(3)
Sm1−C43−C44	165.9(3)		

The structure of **4** is similar to that determined for **1** and **2**; however, in the case of **4**, the samarium center engages in agostic interactions with the methylene carbons of the triethylaluminum groups. The $Sm-C_{methylene}$ distances of 2.627(4) and 2.649(4) Å are similar to the Sm−C bond lengths to the bridging alkyl groups in **2** [2.620(5) and 2.632(5) Å]. The geometry about the agostic carbon atoms (C41, C43) is best described as trigonal bipyramidal, as are the agostic methyl carbons in **1** and **2**. In this case, the Sm−C−C bond angles are 166.8(3)° and 165.9(3)° (Sm1−C41−C42 and Sm1−C43−C44, respectively). The bond lengths and angles determined for the triethylaluminum derivative **4** are virtually identical to those observed for the trimethylaluminum analogue **2**. From this metric data, one would conclude that the substitution of a triethylaluminum group for a trimethylaluminum moiety has a negligible effect on steric congestion about the metal center. While the use of triethylaluminum does not result in longer $Sm-C_{agostic}$ bonds, the effect of using a larger Lewis acid on ligand dynamics in these complexes can be directly observed by ^{1}H NMR spectroscopy (vide supra).

We previously reported the ^{1}H and ^{13}C NMR spectra of (ArO)Sm[(μ-OAr)(μ-Me)$AlMe_2$]$_2$ (**2**); although the spectra were broadened by fluxional processes and the paramagnetism of Sm^{III}, we were able to extract a $^1J_{C\text{-}H}$ coupling constant of 106 Hz for the agostic methyl groups. Lowering the temperature to −90 °C did not result in decoalescence into separate methyl resonances as would be expected for a static structure. Thus, the coupling constant of 106 Hz may be viewed as an average of agostic and nonagostic coupling constants, indicating that the true $^1J_{C\text{-}H}$ coupling determined for the agostic methyl group would be significantly lower. This suggests a strong "classical" Sm···H−C agostic interaction, in which electron density from the C−H bond is donated to the electrophilic metal center.[25,26] This is supported by the infrared spectrum of **2**, which shows a weak intensity ν(C−H) stretch in the solid state and in solution (2728 cm^{-1}). It is possible that a number of different fluxional processes may give rise to the single aluminum-methyl

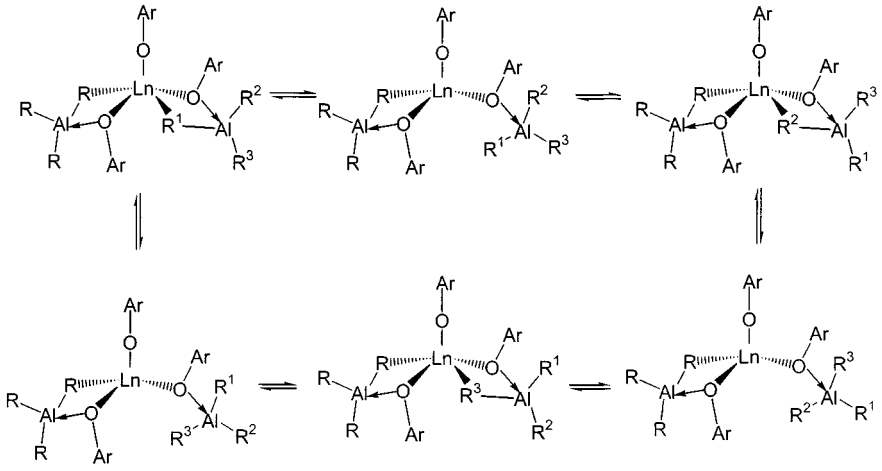

Scheme 1

resonance observed in the variable temperature NMR spectra of **2**: a) rotation about the O−Al bond may serve to average the three aluminum-methyl groups (Scheme 1), b) the trimethylaluminum units may remain fixed to their respective oxygen atoms, but flip between sides of the molecule, roughly defined by the three oxygens (Scheme 2), and c) the two trialkylaluminum moieties may rotate between the three oxygen sites (Scheme 3). In order to potentially distinguish between these three processes, we synthesized the diamagnetic lanthanum analogue in the hope of obtaining spectra that were not broadened by the presence of a paramagnetic metal center.

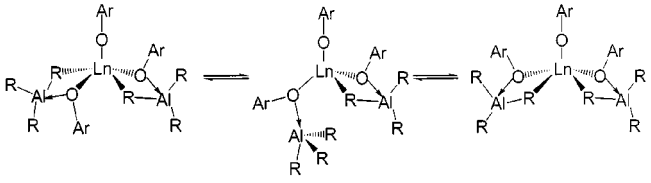

Scheme 2

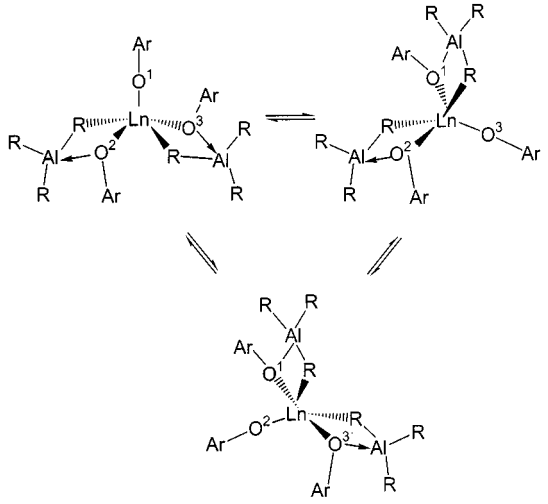

Scheme 3

The ambient temperature ^{1}H NMR spectrum of **1** exhibits a single sharp resonance for the aluminum-methyl groups ($\delta = -0.31$) consistent with rapid bridge-terminal exchange at room temperature (Scheme 1). Lowering the temperature to −90 °C ([D_8]toluene) causes a broadening of the resonance, but decoalescence into separate methyl signals was not observed. The isopropyl methine protons appear as septets in a 2:1 ratio at all temperatures ($\delta = 3.49$ and 3.36). This is consistent with a solution structure that retains the integrity of the aluminum-oxygen bonds at all temperatures, i.e. the trimethylaluminum groups do not exchange between all three aryloxides since this would result in an averaging of the methine proton signals into a single septet (Scheme 3). However, the observation of two methine signals does not allow one to assess whether the fluxional process detailed in Scheme 2 makes a significant contribution to the averaging of the aluminum methyl resonances in solution. In the solid state structure outlined in Figure 1, the four methine protons on the aryloxide ligands associated with the two coordinated trialkylaluminum groups are rendered equivalent both by symmetry (C_2) and by free rotation about the O−C_{ipso} bond; additionally, the two methine protons on the remaining aryloxide ligand are equivalent by symmetry. We note that the operation of a fluxional process such as that described in Scheme 2 would also result in the observation of two methine peaks in a 2:1 ratio, and therefore this piece of data alone does not allow us to determine whether the processes in Scheme 1, Scheme 2, or both, are operating. However, a study of the isopropyl group methyl resonances does allow a distinction to be made. The isopropyl methyl groups in **1** give rise to two doublets in a 2:1 ratio ($\delta = 1.29$ and 1.21); this is consistent with the fluxional process in Scheme 2 being operative at room temperature. Since the isopropyl methyl groups in **1** are diastereotopic in the case of a rigid solution structure, one would expect this region of the ^{1}H NMR spectrum to be more complicated. For example, the methyl groups of the uncomplexed aryloxide unit would result in two doublets of equal intensity. However, dissociation, rotation of the

[(μ-OAr)(μ-Me)AlMe$_2$] fragments about the La−O bonds, and reattachment to the other side of the molecule would generate two pseudo mirror planes (one roughly defined by the three oxygen atoms, and a second plane perpendicular to the first, containing La1, O1 and C1), allowing the four isopropyl methyl groups to appear as a single doublet. Cooling the sample to the low temperature limit (−90 °C) resulted in a loss of resolution such that only a single broad resonance was observed.

The room temperature $^{13}C\{^1H\}$ NMR spectrum of **1** displays a single resonance corresponding to the aluminum-bound methyl groups ($\delta = -0.6$). When the ^{13}C NMR spectrum is collected with proton coupling, a quadruplet is observed with a $^1J_{C\text{-}H}$ coupling constant of 110 Hz. This compares to a coupling constant of 106 Hz determined for the samarium analogue, (ArO)Sm[(μ-OAr)(μ-Me)AlMe$_2$]$_2$ (**2**). As for **2**, a single resonance was evident at all temperatures; thus the value of 110 Hz represents an average of agostic and nonagostic methyl groups. The slightly larger $^1J_{C\text{-}H}$ coupling constant for **1** is consistent with a weaker Ln···H−C agostic interaction and is reflected in the slightly longer Ln−C$_{agostic}$ bond lengths determined for **1**.

As observed previously for **2**, the ^1H NMR spectrum of the samarium triethylaluminum derivative, (ArO)Sm[(μ-OAr)(μ-Et)AlEt$_2$]$_2$ (**4**) consisted of broad, unassignable resonances due to the paramagnetism of samarium. However, in the $^{13}C\{^1H\}$ NMR spectrum, the aluminum-methylene resonances were upfield of the remaining resonances and could be identified by comparison with the spectrum of **2**. In contrast to **2**, the bridge-terminal exchange process is arrested at room temperature; the proton-coupled ^{13}C NMR spectrum displays two triplets in a 2:1 ratio ($\delta = 7.2$ and -5.3). The downfield resonance is twice the intensity of the upfield resonance, and exhibits a normal $^1J_{C\text{-}H}$ coupling constant of 126 Hz. Additionally, this resonance is only slightly broadened, indicating a limited direct contact with the paramagnetic metal center. Conversely, the upfield resonance is significantly broadened ($\Delta\nu_{1/2} = 150$ Hz vs. 50 Hz for **2**) suggesting a carbon atom that resides in a highly relaxed environment. The $^1J_{C\text{-}H}$ coupling constant of 102 Hz is lower than that determined for the agostic methyl groups in **1** or **2**; however, it should be noted that the coupling constant in **4** arises from a static structure, and indicates a weaker interaction than in **1** or **2**, where the $^1J_{C\text{-}H}$ coupling constants of 106 and 110 Hz, respectively, are the averaged values arising from agostic and nonagostic methyl groups. The infrared spectrum of **4** shows a low energy ν(C−H) stretch at 2727 cm^{-1}, which we have previously shown to be consistent with the presence of agostic Ln···C−H interactions in the solid state.[27] In the case of **4**, ^{13}C NMR spectroscopy provides direct evidence for the effect that small changes in sterics can have upon dynamic processes that occur in solution. Whereas X-ray crystallography suggests that the coordination sphere about the samarium center remains virtually unchanged upon going from trimethylaluminum to triethylaluminum, NMR spectroscopy indicates that the triethylaluminum group is sufficiently bulky to retard the fluxional processes postulated to be present in **1** and **2**.

In contrast to **1**, the ^1H and $^{13}C\{^1H\}$ NMR spectra of material isolated in an attempt to prepare (ArO)La[(μ-OAr)(μ-Et)AlEt$_2$]$_2$ (**3**) consist of a large number of resonances that are difficult to assign. From this data, it is evident that **3** is unstable and readily converts to other species in solution or in the solid state. If samples of **3** were left to stand at room temperature for several days, the formation of a dark brown oil and colorless crystals were observed. An X-ray crystallographic study of the crystals determined them to be the aluminum aryloxide species, [Et$_2$Al(OAr)]$_2$ (**5**). An ORTEP representation of the molecular structure of **5** is given in Figure 3. A partial list of bond lengths and angles is available in Table 3.

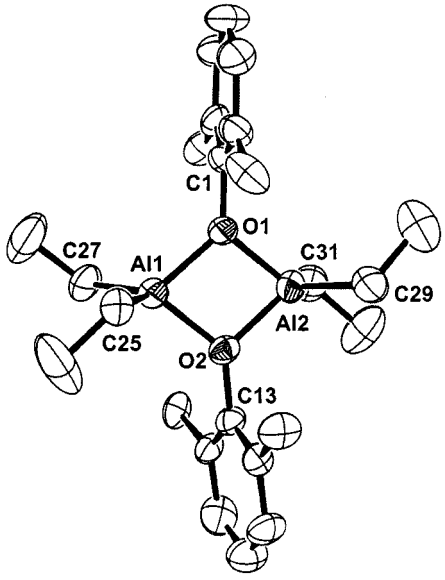

Figure 3. ORTEP view of [Et$_2$Al(OAr)]$_2$ (**5**) drawn with 30% probability ellipsoids; isopropyl methyl groups have been omitted for clarity

Table 3. Selected bond lengths (Å) and angles (deg) for [Et$_2$Al(OAr)]$_2$ (**5**)

Al1−O1	1.855(4)	Al1−O2	1.857(4)
Al1−C25	1.930(7)	Al1−C27	1.948(7)
Al2−O1	1.853(4)	Al2−O2	1.862(4)
Al2−C29	1.916(7)	Al2−C31	1.942(7)
O1−C1	1.420(7)	O2−C13	1.421(6)
O1−Al1−O2	79.65(18)	O1−Al1−C25	116.2(2)
O1−Al1−C27	112.1(3)	O2−Al1−C25	113.2(3)
O2−Al1−C27	116.2(3)	C25−Al1−C27	114.9(3)
O1−Al2−O2	79.56(17)	O1−Al2−C29	112.1(3)
O1−Al2−C31	117.2(3)	O2−Al2−C29	117.3(3)
O2−Al2−C31	112.1(2)	C29−Al2−C31	114.3(3)
C1−O1−Al1	130.5(4)	C1−O1−Al2	129.0(4)
Al1−O1−Al2	100.45(19)	C13−O2−Al1	134.0(4)
C13−O2−Al2	125.9(4)	Al1−O2−Al2	100.04(19)

The crystallographic analysis confirmed the dimeric nature of **5**, in which two aluminum centers are bridged by two phenoxide oxygen atoms. The structure of **5** is analogous to those determined for $[Me_2Al(\mu\text{-}O\text{-}2,6\text{-}i\text{Pr}_2C_6H_3)]_2$ [28] and $[Me_2Al(\mu\text{-}O\text{-}2,4,6\text{-}t\text{Bu}_3C_6H_2)]_2$ [29] and the Al−O and Al−C distances are similar in all three structures. Compound **5** was prepared independently and isolated as colorless crystals from the treatment of $AlEt_3$ with one equivalent of 2,6-diisopropylphenol in toluene after evaporation of the solvent. The isolation of the aluminum-aryloxide dimer **5** from a reaction mixture thought to contain the heterobimetallic species $(ArO)La[(\mu\text{-}OAr)(\mu\text{-}Et)AlEt_2]_2$ implies that aryloxide group transfer is relatively facile in these systems. Samples of $(ArO)La[(\mu\text{-}OAr)(\mu\text{-}Me)AlMe_2]_2$ (**1**) and $(ArO)Sm[(\mu\text{-}OAr)(\mu\text{-}Me)AlMe_2]_2$ (**2**) were re-examined by NMR spectroscopy and found to contain small amounts ($< 5\%$) of the previously reported aluminum phenoxide species, $[Me_2Al(\mu\text{-}O\text{-}2,6\text{-}i\text{Pr}_2C_6H_3)]_2$. Heating samples of **1** or **2** to 80 °C overnight resulted in an increase in the intensity of the signals due to $[Me_2Al(\mu\text{-}O\text{-}2,6\text{-}i\text{Pr}_2C_6H_3)]_2$, and the formation of a third, unidentified species (presumably a Ln dialkyl derivative). We suggest that a ligand redistribution reaction such as that detailed in Scheme 4 is occurring: original addition of four equivalents of trialkylaluminum to the π-arene-bridged dimers $[Ln(OAr)_3]_2$ results in the monomeric bis-trialkylaluminum adducts $(ArO)Ln[(\mu\text{-}OAr)(\mu\text{-}R)AlR_2]_2$ which are held together by dative O→Al bonds (I). Due to the steric constraints of the bulky aryloxide groups, only two trialkylaluminum groups per metal center are complexed. The electrophilic lanthanide center engages in further interactions to satisfy its Lewis acidity in the form of a π-bonding interaction with the remaining uncomplexed aryloxide group, and two agostic interactions with the methyl or methylene carbons of the trialkylaluminum units (II). Due to the oxophilicity of aluminum, and the weakened $Al-C_{agostic}$ bonds in II, an alkyl group from each aluminum atom is transferred to the lanthanide center as two formal aluminum-oxygen bonds are formed (III). The bis-trialkylaluminum adduct then separates into three discrete species (IV) which then recombine to form one equivalent of the dimeric aluminum-aryloxide species $[R_2Al(OAr)]_2$ (V) and a lanthanide dialkyl species (VI), which is most likely unstable and reacts further to form other unidentified decomposition products.

In the sense that II is an intermediate in the ligand redistribution reaction of $(ArO)Ln[(\mu\text{-}OAr)(\mu\text{-}R)AlR_2]_2$ to form $[R_2Al(OAr)]_2$ and "R_2LnOAr", the crystal structures of $(ArO)La[(\mu\text{-}OAr)(\mu\text{-}Me)AlMe_2]_2$ (**1**), $(ArO)Sm[(\mu\text{-}OAr)(\mu\text{-}Me)AlMe_2]_2$ (**2**) and $(ArO)Sm[(\mu\text{-}OAr)(\mu\text{-}Et)AlEt_2]_2$ (**4**) may be viewed as "snapshots" of these intermediates, where the migration of the methyl and/or ethyl groups from the aluminum to the metal center has been arrested.[30]

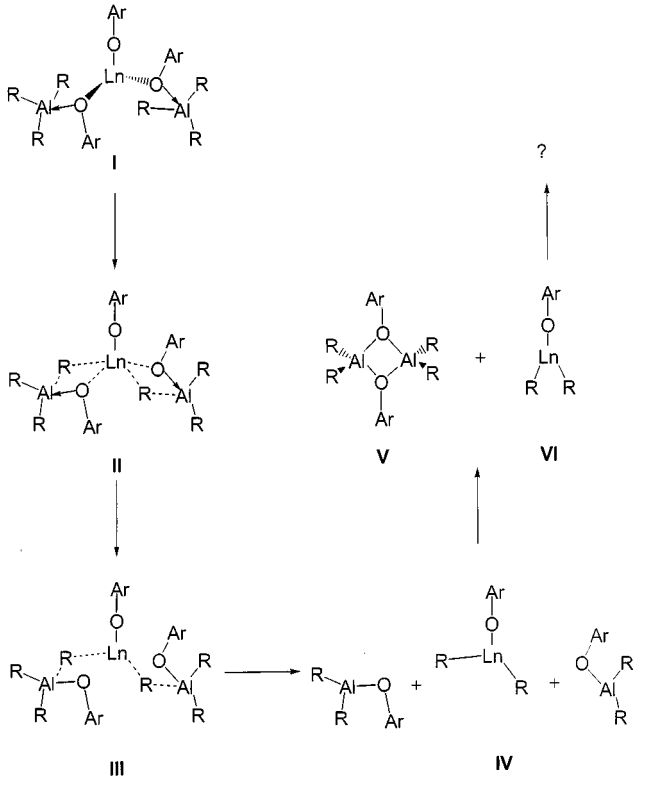

Scheme 4

Conclusions

The synthesis of heterobimetallic complexes of the lanthanides is easily achieved by the addition of trialkylaluminum reagents to the dimeric starting materials, $[Ln(OAr)_3]_2$. By utilizing the bulky 2,6-ddiisopropylphenoxide ligand, adduct formation stops after the addition of two trialkylaluminum units per metal center, which contrasts with trialkylaluminum adducts of the smaller alkoxide, $Ln[(\mu\text{-}Ot\text{Bu})(\mu\text{-}Me)AlMe_2]_3$. These heterobimetallic complexes appear to lie somewhere on a continuum between classical Ln···H−C interactions and Ln···C−X bonding modes which have recently been described. The staggered hydrogens on the five-coordinate agostic carbons and the elongated Al−C bonds in the crystal structures of **1** and **4** support the donation of electron density from the aluminum-carbon bond to the lanthanide center; however, the reduced C−H coupling constants and the lowered infrared stretching frequencies are consistent with a more conventional γ-C−H···Ln interaction. The averaging of the trialkylaluminum methyl groups in the ambient temperature NMR spectra of **1** is likely a result of two separate processes: 1) rotation about the O−Al bond, and 2) the flipping of trialkylaluminum units to opposite sides of the molecule while remaining bound to the aryloxide oxygen atoms. The effect of the larger trialkylaluminum group in **4** is evidenced by ^{13}C NMR spectroscopy, where the bridging and terminal methylene groups give rise to distinct resonances. These adducts readily undergo alkyl/aryloxide group transfer upon thermolysis; thus the crystals structures of **1** and **4** may not only be viewed as examples of lanthanide centers engaging in agostic interactions with remote alkyl groups, but also as intermediates in the transfer of alkyl groups from an aluminum atom to a highly electrophilic lanthanide center.

Experimental Section

General Remarks: All manipulations were carried out under an inert atmosphere of oxygen-free UHP grade argon using standard Schlenk techniques or under oxygen-free helium in a Vacuum Atmospheres glovebox. $AlMe_3$ (2.0 M hexane solution) and $AlEt_3$ (1.9 M toluene solution) were purchased from Aldrich and used as received. 2,6-diisopropylphenol was purchased from Aldrich, distilled over sodium and crystallized at −40 °C prior to use. $[Sm(OAr)_3]_2$,[1] $[La(OAr)_3]_2$ [2] and $[Me_2Al(OAr)]_2$ [28] were prepared according to literature procedures. Hexane and toluene were deoxygenated by passage through a column of supported copper redox catalyst (Cu-0226 S) and dried by passing through a second column of activated alumina. Hexamethyldisiloxane was distilled over sodium benzophenone and degassed prior to use. $[D_6]$benzene and $[D_8]$toluene were degassed, dried over Na-K alloy, and trap-to-trap distilled before use. ^{1}H NMR spectra were recorded on a Bruker AMX 500 spectrometer at ambient temperature; chemical shifts are given relative to residual $[D_5H]$benzene (δ = 7.15) or $[D_7H]$toluene (δ = 2.09). ^{13}C NMR chemical shifts are given relative to $[D_6]$benzene (δ = 128.39) or $[D_8]$toluene (δ = 20.4). Infrared spectra were recorded on a Nicolet Avatar 360 FT-IR spectrometer; solid-state spectra were taken as Nujol mulls between KBr plates, while solution spectra were recorded as benzene solutions vs. a solvent blank in KBr cells. Elemental analyses were performed on a Perkin−Elmer 2400 CHN analyzer. Elemental analysis samples were prepared and sealed in tin capsules in a glovebox prior to combustion.

(ArO)La[(μ-OAr)(μ-Me)AlMe$_2$]$_2$ (1): $AlMe_3$ (0.75 mL of a 2.0 M solution in hexane, 1.50 mmol) was added to a toluene solution of $[La(OAr)_3]_2$ (500 mg, 0.37 mmol). The mixture was stirred at room temperature for 30 minutes and then filtered through a Celite pad. The solvent was removed under vacuum and the sticky residue was washed with a minimum of hexane. Slow evaporation of a saturated toluene solution yielded waxy, colorless crystals (420 mg, 68% yield). ^{1}H NMR (500 MHz, $[D_8]$toluene): δ = −0.31 (s, 18 H, Al*Me$_3$*), 1.21 and 1.29 (2:1 d, $^3J_{H\text{-}H}$ = 6.6 Hz, 36 H, CH*Me$_2$*), 3.36 and 3.49 (1:2 sept, $^3J_{H\text{-}H}$ = 6.6 Hz, 6 H, C*H*Me$_2$), 6.70−7.20 (overlapping m, 9 H, *m,p*-H). ^{13}C{^{1}H} NMR (125 MHz, $[D_8]$toluene): δ = −0.6 (Al*Me$_3$*), 24.5, 24.8 and 24.9 (isopropyl methyl), 27.6 and 28.2 (isopropyl methine), 121.2, 123.0, 123.8 and 124.2 (phenyl *C*H), 136.7, 139.8, 147.0 and 159.1 (tertiary phenyl). Selected ^{13}C NMR spectroscopic data (125 MHz, $[D_8]$toluene): δ = −0.6 (q, $^1J_{C\text{-}H}$ = 110 Hz, Al*Me$_3$*). IR (Nujol): $\tilde{\nu}$ = 2783 cm^{-1} (m), 2725 (m), 1588 (m), 1364 (s), 1322 (s), 1252 (s), 1197 (s), 1097 (s), 1054 (m), 1041 (s), 933 (s), 886 (s), 835 (s), 797 (s), 758 (s), 703 (s), 628 (s). $C_{42}H_{69}Al_2LaO_3$ (814.9): calcd. C 61.91, H 8.53; found C 60.97, H 8.24.

(ArO)La[(μ-OAr)(μ-Et)AlEt$_2$]$_2$ (3): $AlEt_3$ (0.75 mL of a 1.9 M solution in toluene, 1.50 mmol) was added to a toluene solution of $[La(OAr)_3]_2$ (500 mg, 0.37 mmol). The mixture was stirred at room temperature for 90 minutes. The solvent was removed under vacuum and the residue was washed with a minimum of hexane to yield a colorless oil. Over a period of several days, the residue changed into a mixture of a dark red oil and large colorless crystals. X-ray crystallography indicated that the crystals consisted of $[Et_2Al(OAr)]_2$ (**5**). No discrete lanthanum-containing species were identified.

(ArO)Sm[(μ-OAr)(μ-Et)AlEt$_2$]$_2$ (4): $AlEt_3$ (0.47 mL of a 1.9 M solution in toluene, 0.91 mmol) was added to a toluene solution of $[Sm(OAr)_3]_2$ (310 mg, 0.23 mmol), causing an immediate color change from yellow to orange. The mixture was stirred at room temperature for 90 minutes. The solvent was removed under vacuum and the sticky residue was washed with a minimum of hexane. Slow evaporation of a saturated hexamethyldisiloxane solution yielded small orange crystals (340 mg, 80% yield). Selected ^{13}C NMR spectroscopic data (125 MHz, $[D_6]$benzene): δ = 7.2 (t, $^1J_{C\text{-}H}$ = 126 Hz, 4C, nonagostic Al*C*H$_2$), −5.3 (t, $^1J_{C\text{-}H}$ = 102 Hz, $\Delta\nu_{1/2}$ = 150 Hz, 2C, agostic Al*C*H$_2$). IR (Nujol): $\tilde{\nu}$ = 2785 cm^{-1} (w), 2727 (w), 1588 (m), 1424 (s), 1391 (s), 1317 (m), 1243 (m), 1186 (m), 1181 (m), 1088 (m), 1047 (w), 1030 (m), 965 (w), 948 (m), 924 (w), 883 (m), 855 (m), 825 (m), 785 (s), 735 (s), 686 (w), 673 (m), 654 (w). $C_{48}H_{81}Al_2O_3Sm$ (910.5): calcd. C 63.32, H 8.97; found C 61.69, H 9.36.

[Et$_2$Al(OAr)]$_2$ (5): $AlEt_3$ (1.00 mL of a 1.9 M solution in toluene, 1.90 mmol) was added to a toluene solution of 2,6-diisopropylphenol (340 mg, 1.90 mmol). Gas evolution was apparent immediately. The reaction mixture was stirred for 1 h, and the solvent removed under vacuum to yield a white, crystalline solid (420 mg, 84% yield). ^{1}H NMR (500 MHz, $[D_6]$benzene): δ = 0.41 (q, $^3J_{H\text{-}H}$ = 8.2 Hz, 8 H, CH$_3$C*H$_2$*Al), 1.01 (t, $^3J_{H\text{-}H}$ = 8.2 Hz, 12 H, C*H$_3$*CH$_2$Al), 1.30 (d, $^3J_{H\text{-}H}$ = 6.8 Hz, 24 H, CH*Me$_2$*), 3.72 (sept, $^3J_{H\text{-}H}$ = 6.8 Hz, 4 H, C*H*Me$_2$), 6.95−7.04 (overlapping m, 6 H, *m,p*-H). ^{13}C{^{1}H} NMR (125 MHz, $[D_6]$benzene): δ = 0.8 (CH$_3$*C*H$_2$Al), 10.6 (*C*H$_3$CH$_2$Al), 25.9 (*C*HMe$_2$), 27.2 (CH*Me$_2$*), 125.7 and 125.9 (phenyl *C*H), 141.0 (*o*-phenyl), 145.8 (*ipso*-phenyl). IR (Nujol): $\tilde{\nu}$ = 1445 cm^{-1} (s), 1411 (m), 1383 (m), 1377 (m), 1344 (w), 1320 (w), 1260 (m), 1245 (w), 1189 (m), 1162 (s), 1097 (s), 1054 (m), 1041 (w), 972 (m), 949 (m), 933 (m), 884 (m), 833 (s), 800 (m), 758 (s), 693 (s), 668 (s), 633 (s), 610 (s). $C_{32}H_{54}Al_2O_2$ (524.7): calcd. C 73.25, H 10.37; found C 72.31, H 11.04.

X-ray Crystallographic Studies: Crystals of **1**, **4**, and **5** were mounted on a thin glass fiber using a small dot of silicone grease. The crystals were then immediately placed on a Bruker P4/CCD/PC diffractometer, and cooled to 203 K using a Bruker LT-2 temperature device. The data were collected using a sealed, graphite monochromatized Mo-K_α X-ray source. A hemisphere of data was collected using a combination of and ω scans, with 30-second frame exposures and 0.3° frame widths. Data collection and initial indexing and cell refinement was handled using SMART[31] software. Frame integration and final cell parameter calculations were carried out using SAINT[32] software. The data were corrected for absorption using the SADABS[33] program. Decay of reflection intensity was not observed.

The structures were solved using Direct methods and difference Fourier techniques. The initial solution revealed all non-hydrogen atom positions. The methyl hydrogen atom positions for C37 and C40 (**1**) were found on the difference map and refined with their isotropic temperature factors set to 0.08 Å^2. The methylene hydrogen atom positions for C41 and C43 (**4**) were also found and refined as described above. All other hydrogen atoms positions were idealized, C−H = 0.93 Å (aromatic), 0.96 Å (methyl), 0.98 Å (methine) and 0.97 Å (methylene). The hydrogen atoms were refined using a riding model, with isotropic temperature factors fixed at 1.5 (methyl) or 1.2 (all others) times the equivalent isotropic U of the atom they are bonded to. The final refinement[34] included anisotropic temperature factors on all atoms. Structure solution, refinement, graphics, and creation of publication materials were performed using SHELXTL NT.[35] Additional details of data collection and structure refinement are listed in Table 4. Crystallographic data (excluding structure factors) for the structures reported in this paper have been deposited with the Cambridge Crystallographic Data Centre as supplementary publication nos. CCDC-171086 (**1**), CCDC-171087 (**4**) and CCDC-171088 (**5**). Cop-

Table 4. Crystallographic data

Compound	**1**	**4**	**5**
Formula	$C_{42}H_{69}Al_2LaO_3$	$C_{48}H_{81}Al_2O_3Sm$	$C_{32}H_{54}Al_2O_2$
Molecular Weight	814.84	910.44	524.71
Temperature, K	203(2)	203(2)	203(2)
Crystal System	Orthorhombic	Orthorhombic	Triclinic
Space Group	$P2_12_12_1$	*P*bca	$P\bar{1}$
Crystal Size, mm	0.16 × 0.16 × 0.12	0.12 × 0.12 × 0.31	0.28 × 0.20 × 0.12
a, Å	11.708(2)	19.318(1)	9.496(4)
b, Å	18.416(4)	20.150(1)	10.183(4)
c, Å	20.949(4)	26.280(1)	18.794(7)
α, °	90	90	90.06(1)
β, °	90	90	92.394(7)
γ, °	90	90	114.976(6)
V, Å^3	4516.8(15)	10229.8(9)	1645.6(11)
Z	4	8	2
D_{calc}, g/mL	1.198	1.182	1.059
Absorption coeffiecient, mm^{-1}	1.017	1.217	0.112
F(000)	1712	3848	576
Theta range, °	1.47 to 25.35	1.6 to 23.4	1.08 to 22.46
Total reflections	29540	36958	7343
Independent reflections	8251	7363	3969
GOF	1.103	1.439	1.334
R*1*	0.0469	0.0353	0.1013
*wR*2	0.0798	0.0719	0.2061

ies of the data can be obtained free of charge on application to CCDC, 12 Union Road, Cambridge CB2 1EZ, UK [Fax: (internat.) + 44-1223/336-033; E-mail: deposit@ccdc.cam.ac.uk].

Acknowledgments

We acknowledge the Office of Basic Energy Sciences, the Division of Chemical Sciences and the U. S. Department of Energy for funding (via the LDRD ER program). Los Alamos National Laboratory is operated by the University of California for the U.S. Department of Energy under Contract W-7405-ENG-36.

[1] D. M. Barnhart, D. L. Clark, J. C. Gordon, J. C. Huffman, R. L. Vincent, J. G. Watkin, B. D. Zwick, *Inorg. Chem.* **1994**, *33*, 3487−3497 and references therein.
[2] R. J. Butcher, D. L. Clark, S. K. Grumbine, R. L. Vincent-Hollis, B. L. Scott, J. G. Watkin, *Inorg. Chem.* **1995**, *34*, 5468−5476 and references therein.
[3] D. L. Clark, S. K. Grumbine, B. L. Scott, J. G. Watkin, *Organometallics* **1996**, *15*, 949−957 and references therein.
[4] P. B. Hitchcock, M. F. Lappert, A. Singh, *J. Chem. Soc., Chem. Commun.* **1983**, 1499−1501.
[5] G. H. Qi, Y. Lin, J. Hu, Q. Shen, *Polyhedron* **1995**, *14*, 413−415.
[6] K. G. Caulton, L. G. Hubert-Pfalzgraf, *Chem. Rev.* **1990**, *90*, 969−995.
[7] W. J. Evans, T. J. Boyle, J. W. Ziller, *J. Organomet. Chem.* **1993**, *462*, 141−148.
[8] W. J. Evans, T. J. Boyle, J. W. Ziller, *J. Am. Chem. Soc.* **1993**, *115*, 5084−5092.
[9] P. Biagini, G. Lugli, L. Abis, R. Millini, *J. Organomet. Chem.* **1994**, C16−C18.
[10] W. J. Evans, M. A. Ansari, J. W. Ziller, *Polyhedron* **1997**, *16*, 3429−3434.
[11] H. Sinn, W. Kaminsky, *Adv. Organomet. Chem.* **1980**, *18*, 99−149.
[12] G. Wilkinson, F. G. A. Stone, E. W. Abel, *Comprehensive Organometallic Chemistry, Vol. 3*, Pergamon Press, Oxford, **1982**, p. 475.
[13] L. Porri, A. Giarrusso, in *Comprehensive Polymer Science, Vol. 4* (Eds.: G. C. Eastmond, A. Ledwith, S. Russo, P. Sigwalt), Pergamon Press, Oxford, **1989**, p. 53.
[14] L. G. Hubert-Pfalzgraf, *New J. Chem.* **1987**, *11*, 663−675.
[15] D. C. Bradley, *Chem. Rev.* **1989**, *89*, 1317−1322.
[16] D. C. Bradley, *Polyhedron* **1994**, *13*, 1111−1121.
[17] L. G. Hubert-Pfaltzgraf, *New J. Chem.* **1995**, *19*, 727−750.
[18] R. C. Mehrotra, A. Singh, *Chem. Soc. Rev.* **1996**, 1−14.
[19] J. C. Gordon, G. R. Giesbrecht, J. T. Brady, D. L. Clark, D. W. Keogh, B. L. Scott, J. G. Watkin, *Organometallics* **2001**, in press.
[20] [20a] The difference in ionic radii between lanthanum (1.17 Å) and samarium (1.10 Å) is 0.07 Å. [20b] Taking this into account, the Ln−C distances in **1** are about 0.085 Å longer than those found in the samarium derivative **2**. [20b] R. D. Shannon, *Acta Crystallogr., Sect. A* **1976**, *32*, 751−767.
[21] P. B. Hitchcock, M. F. Lappert, R. G. Smith, R. A. Bartlett, P. P. Power, *Chem. Commun.* **1988**, 1007−1009.
[22] H. van der Heijden, C. J. Schaverien, A. G. Orpen, *Organometallics* **1989**, *8*, 255−258.
[23] C. J. Schaverien, G. J. Nesbitt, *J. Chem. Soc., Dalton Trans.* **1992**, 157−167.
[24] W. T. Klooster, L. Brammer, C. J. Schaverien, P. H. M. Budzelaar, *J. Am. Chem. Soc.* **1999**, 1381−1382.
[25] M. Brookhart, M. L. H. Green, L. L. Wong, *Prog. Inorg. Chem.* **1988**, *36*, 1−124.
[26] J. Eppinger, M. Spiegler, W. Hieringer, W. A. Herrmann, R. Anwander, *J. Am. Chem. Soc.* **2000**, *122*, 3080−3096.
[27] D. M. Barnhart, D. L. Clark, J. C. Gordon, J. C. Huffman, J.

G. Watkin, B. D. Zwick, *J. Am. Chem. Soc.* **1993**, *115*, 8461−8462.
[28] A. V. Firth, J. C. Stewart, A. J. Hoskin, D. W. Stephan, *J. Organomet. Chem.* **1999**, *591*, 185−193.
[29] B. Cetinkaya, P. B. Hitchcock, H. A. Jasim, M. F. Lappert, H. D. Williams, *Polyhedron* **1990**, *9*, 239−243.
[30] For a similar example of an arrested methyl-group migration, see: D. L. Clark, J. C. Gordon, J. C. Huffman, J. G. Watkin, B. D. Zwick, *Organometallics* **1994**, *13*, 4266−4270.
[31] SMART Version 4.210, **1996**, Bruker Analytical X-ray Systems, Inc., Madison, Wisconson, 53719.
[32] SAINT Version 4.05, **1996**, Bruker Analytical X-ray Systems, Inc., Madison, Wisconson, 53719.
[33] SADABS, first release, George Sheldrick, University of Göttingen, Germany.
[34] $R_1 = \Sigma||F_o|-|F_c||/\Sigma|F_o|$ and $R_{2w} = \{\Sigma[w(F_o^2 - F_c^2)^2]/\Sigma[\omega(F_o^2)^2]\}^{1/2}$; $w = 1/[\sigma^2(F_o^2) + (aP)^2]$, where $a = 0.0393(2)$, $0.0285(3)$, and $0.0719(4)$.
[35] SHELXTL NT Version 5.10, **1997**, Bruker Analytical X-ray Instruments, Inc., Madison, Wisconsin, 53719.

Received September 18, 2001
[I01367]